J Paleolimnol
DOI 10.1007/s10933-008-9235-1

ORIGINAL PAPER

Depositional history of the Miocene Lake Sinj (Dinaride Lake System, Croatia): a long-lived hard-water lake in a pull-apart tectonic setting

Oleg Mandic · Davor Pavelić · Mathias Harzhauser · Jožica Zupanič · Doris Reischenbacher · Reinhard F. Sachsenhofer · Neven Tadej · Alan Vranjković

Received: 19 December 2007 / Accepted: 30 June 2008

Abstract Early Miocene transpressional wrenching yielded a series of NW–SE-elongated pull-apart basins in the Dinarides of Croatia and Bosnia and Herzegovina. They accommodated a huge lake system that gave rise to spectacular endemic mollusk radiation. Lake Sinj, moderately sized at 342 km^2, flooded the south-westernmost basin of this system. Due to the karstic environment, the hard-water, alkaline, long-lived lake developed a sediment infill with an average thickness of 370 m, dominated by authigenic limestone. The studied section represents the upper third of the basinal infill and provides detailed insights into the critical period of the lake and of the basinal evolution during the final stages of its filling. It comprises two large-scale, shallowing-upward cycles, both starting with fossil-poor limestones, gradually passing into coal-bearing carbonate rocks and coal seams. The fossil-poor intervals are interpreted as phases of repetitive acidification events due to changing lake level, which induced periodic drying and flooding of the uppermost littoral zone inhabited by starfruit (*Damasonium*) meadows. The flooding of the aerated, limy mud plain introduced H+ ions from organic-matter decay reactions into the shallow lake. This decreased its pH level, with catastrophic consequences for its biota. The ecosystem then stabilized during the orbitally-forced, dry climate phases. Based on the mollusk record, streams still influenced the marginal lake environment and rich organic-matter production created swamps and mires. The onset of mollusk radiation in the section correlates with stabilized lake alkalinity, as indicated by the disappearance of starfruits, ongoing authigenic carbonate production and by coal seams representing textbook examples for coal formation in alkaline environments. The inferred basinal setting fits well with the pull-apart basin model, pointing to the

O. Mandic (✉) · M. Harzhauser
Geological-Paleontological Department, Natural History Museum Vienna, Burgring 7, 1010 Wien, Austria
e-mail: oleg.mandic@nhm-wien.ac.at

M. Harzhauser
e-mail: mathias.harzhauser@nhm-wien.ac.at

D. Pavelić · N. Tadej · A. Vranjković
Faculty of Mining, Geology and Petroleum Engineering, University of Zagreb, Pierottijeva 6, 10000 Zagreb, Croatia
e-mail: dpavelic@rgn.hr

N. Tadej
e-mail: ntadej@rgn.hr

A. Vranjković
e-mail: avranjko@rgn.hr

J. Zupanič
Faculty of Science, University of Zagreb, Horvatovac bb, 10000 Zagreb, Croatia
e-mail: jzupanic@geol.pmf.hr

D. Reischenbacher · R. F. Sachsenhofer
Department of Geological Sciences, University of Leoben, Peter-Tunner-Strasse 5, 8700 Leoben, Austria
e-mail: reinhard.sachsenhofer@mu-leoben.at

presence of an extended shallow ramp in front of a steep, fault-induced hillside of the hinterland.

Keywords Long-lived lakes · Hard-water lakes · Pull-apart basins · Authigenic carbonates · Coals · Orbitally-forced cycles

Introduction

Lacustrine carbonates are the focus of increasing interest because they record details on environments and regional evolution (review in Tucker and Wright 1990; Anadon et al. 1991). This is because conditions for carbonate deposition in lakes strongly depend on climate, lake hydrology, tectonics, and morphology. Carbonate lacustrine systems are therefore much less stable than their marine counterparts. Lacustrine carbonates are also important because they contain mineral deposits, including coal, and comprise source rocks for hydrocarbons (Tucker and Wright 1990; Anadon et al. 1991).

This work describes the features and evolution of a Miocene carbonate lake and interprets the relevant controlling factors. Beyond the influence of factors such as climate and tectonics, the features of this lake were determined by its occurrence in a karst realm. This karst area belongs to the External Dinarides, which are dominated by Mesozoic and Paleogene carbonates. We document almost exclusive calcite deposition in this lake and elaborate the importance of biological processes for the origin and character of several limestone facies. We also discuss the origin of the alternation of limestones and coal, and relate them to cyclic climate changes.

Geological setting

The studied deposits are located in SE Croatia and belong to the infill of the Sinj Basin on the SE margin of the External Dinarides, bounded to the southwest by the Adriatic block. The basin is elongated, NW–SE striking, rhomboidal, and measures 38 × 9 km; it can be interpreted as a pull-apart tectonic structure. It was formed within the Western Thrust Belt of the Dinarides during the Early Miocene due to transpressional wrenching caused by northward oblique-slip motions of the underthrusting Adriatic block (Tari 2002). That transpressional regime initiated numerous other synchronous NW–SE striking pull-apart basins distributed across the Dinarides. Together, these basins accommodated a system of freshwater environments termed the Dinaride Lake System (Krstić et al. 2003). That long-lived lake environment experienced a spectacular evolution of lacustrine mollusks, preceding the better known radiation event in neighboring Lake Pannon by 5–10 Ma. (Harzhauser and Mandic 2008a, b). The Dinaride Lake System represented an independent paleogeographic and paleobiogeographic entity restricted to the northern part of the Dinarian-Anatolian Island, which acted as geographic barrier between the Paratethys and proto-Mediterranean (Fig. 1).

The Sinj Basin is located in the western, marginal part of the Dinaride Western Thrust Belt termed the Frontal Thrust (Tari 2002). The Dinaride Western Thrust Belt predominantly comprises carbonate rocks originating from the Mesozoic to early Cenozoic Dinaride carbonate platform. It also includes imbricates from the synchronous Adriatic carbonate platform. With the start of compressional tectonics

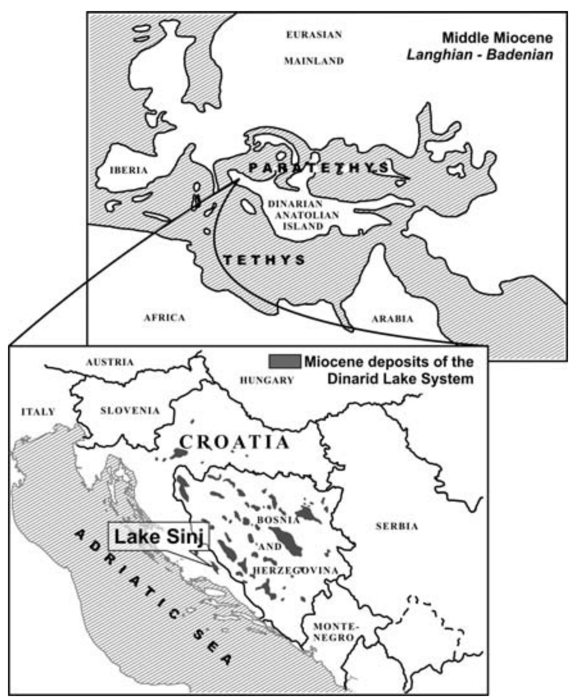

Fig. 1 Paleogeographic setting of Lake Sinj (modified after Harzhauser and Mandic 2008a)

during the Eocene, which led to the formation of the SW-vergent Western Thrust Belt, the platform turned briefly into a foredeep with flysch and molasse sedimentation (Promina Formation). It finally emerged during the Oligocene. The main decollement horizon is formed by the base of the carbonate platform comprising Permo-Triassic pelitic and evaporitic rocks. At the start of transpressional tectonics in the Lower Miocene, which generated the Sinj Basin, the area was already continentalised.

The rim of the Sinj Basin comprises Triassic to Eocene platform carbonate rocks. Only the western margin includes clastic rocks of the Eocene-Oligocene Promina Formation and the Lower Triassic Muć Formation (Papeš et al. 1984; Marinčić et al. 1969). The basin itself is affected in its western part by the doming of Permo-Triassic evaporites (Raić et al. 1984).

The succession of Miocene freshwater deposits in the Sinj Basin consists of dominant limestones, coal intercalations, and a few tuff beds. This has been mapped and studied in detail by Kerner (1916b, c), Šušnjara and Šćavničar (1974) and Šušnjara and Sakač (1988). Accordingly, three main lithological units are present within the succession (average thickness 370 m; Fig. 2). The basal unit ("Basal beds") comprises varicolored marls in the west and "Older coal-bearing beds" and marls with dreissenid bivalves in the eastern part of the basin. The difference is interpreted to reflect the different lithological character of the basement rocks. The middle unit is formed throughout by clayey limestones and limy marls. The upper unit is termed the "Younger coal-bearing beds". The fossiliferous limy marls contain an up to 4-m-thick coal seam and several thinner coal intercalations as well as dreissenid marl subunits. The "Younger coal-bearing beds" are especially well developed along the southwestern basinal margin, where they onlap transgressively (Šušnjara and Sakač 1988). Our study encompasses a 138-m-thick section in the western part of the basin representing the "Younger coal-bearing beds". A similar section has been studied in a north-neighboring east-west striking gully by Kerner (1905a). From

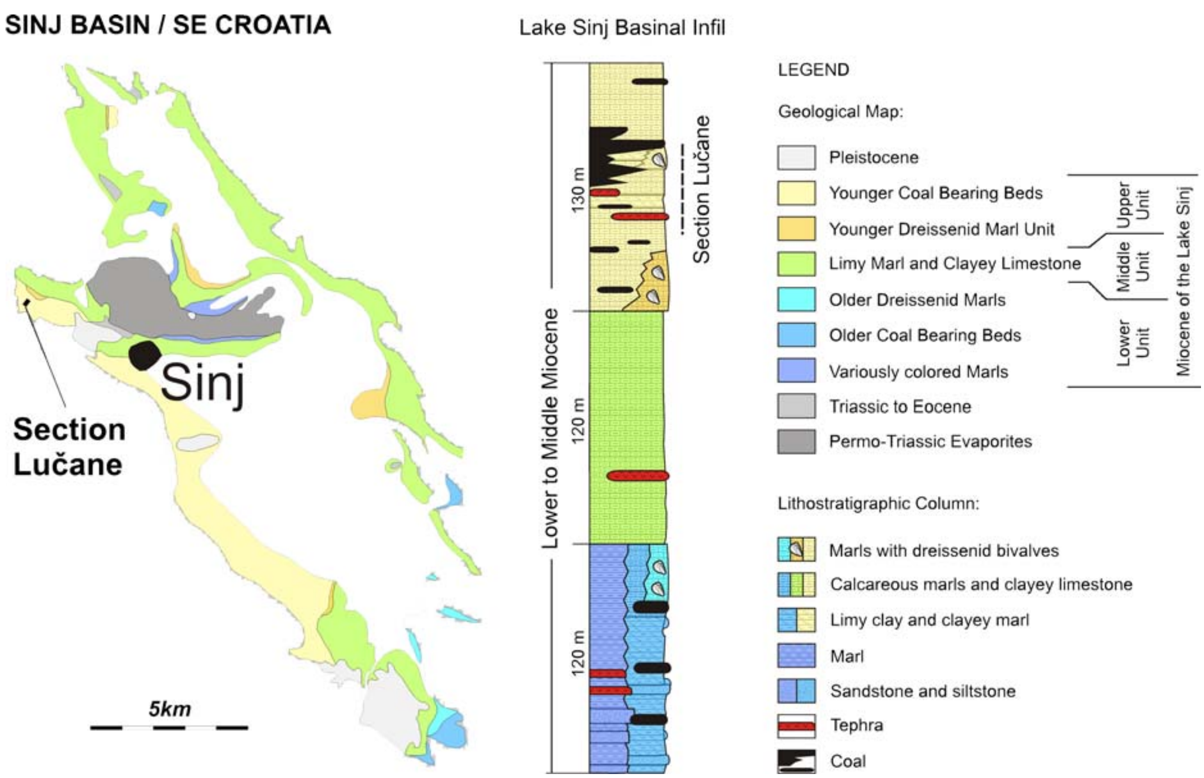

Fig. 2 Geological map of the Sinj Basin showing the classification and distribution of Miocene infill lithostratigraphic units (modified after Šušnjara and Sakač 1988)

the studied section, Olujić (1936, 1999) investigated the evolutionary history of several *Melanopsis* and *Prososthenia* gastropod species. The species-rich, highly endemic, lacustrine mollusk fauna near the section as well as from other Sinj Basin localities has been described in numerous studies such as Neumayr (1869), Brusina (1874, 1878, 1882, 1892, 1897), Olujić (1936, 1999), and Kochansky-Devidé and Slišković (1978). All document the existence of prominent speciation and radiation processes within the lake (Harzhauser and Mandic 2008a, b).

Age and duration of deposition

The uppermost Lake Sinj deposits bear highly endemic dreissenid bivalves such as *Mytilopsis aletici*. Kochansky-Devidé and Slišković (1978) regard these as representing the youngest deposits of the Dinaride Lake System (DLS). The studied section intersects the *M. aletici* zone. The absence of such fauna in the adjoining Upper Miocene Lake Pannon reflects its younger age. This resulted in a tentative correlation of topmost DLS deposits with the Middle Miocene or, in terms of Central Paratethys chronostratigraphy, with the Late Badenian to Early Sarmatian. Data from large mammal remains point to an even older age of the latest DLS deposits, i.e. latest Early Miocene.

Accordingly, in the coal layer at 135 m, a large mammal fauna including *Gomphotherium angustidens* and *Conochyus olujici* was collected by mine workers in the 1930s (J. Radovčić in Olujić 1999, Bernor et al. 2004). At slightly younger stratigraphic position in the coal layers of Raduša, SW Sinj, *G. angustidens* is accompanied by *Brachypotherium brachypus*, pointing to latest Early Miocene to earliest Late Miocene age (Takšić 1968; Jurišić-Polšak 1999). Based on the evolutionary stage inference for *C. olujici*, Bernor et al. (2004) narrowed the stratigraphic range for the topmost coal layer at the Lučane section to the latest Early Miocene interval between ca. 17 Ma and maximally 16.1 Ma.

Most recently, however, the radiometric data for a tephra layer originally recorded by Bulić (1999) and found in the studied section at 39.3 m (Figs. 2 and 3), did not confirm the former inference (Jurišić-Polšak and Bulić 2007: 60). Hence, the tephra layer, positioned 96 m below the large mammal bed, is considered by the authors to be earliest Middle Miocene, unfortunately without numerical evidence. Nevertheless that datum fits very well with the magnetostratigraphic pattern revealed for the section, where most of the section is reversed and only the top part is within a normal interval (Mandic et al. 2007). Consequently, the studied section at Lučane and the topmost part of the Sinj Basin infill must be younger than the Middle Miocene base (16 Ma), but older than ca. 15 Ma.

The results of cyclostratigraphic studies for the Lučane section indicated a sedimentation rate of about 0.2 mm/a by calibrating two shallowing-upward limestone/coal cycles with two 400-ka. eccentricity periods (Mandic et al. 2006). That finding coincides with sediment accumulation rates presented in Cohen (2003).

The lower part of Lake Sinj deposits correlates tentatively with the Early Miocene based on mass occurrence of *Ceratostriotes sinjanus* (Kerner 1905b). That plant is rare elsewhere, but is abundant in a single Early Miocene horizon of the Central Paratethys located in NE Austria and SW Czech Republic (Bužek 1982; Meller and Bergen 2003), dated there to the Late Ottnangian (app. 17.5 Ma after Rögl et al. 2004).

The longevity of Lake Sinj is indicated additionally by its conspicuously high species richness and the extreme endemicity of that fauna (98%; cf. Harzhauser and Mandic 2008a, b). A review of literature data found more than 100 mollusk species and subspecies present in those deposits.

Methods

The composition, structures, and textures of limestones were studied using polished sections and slabs, and thin sections. The observed features were used to define several limestone facies, although they could not always be identified in the field. Color was determined using the Munsell Color Chart (Goddard et al. 1963). Feigel′s solution was used to identify aragonite in thin sections.

Whole-rock X-ray powder diffractometer analyses were made at the Faculty of Mining, Geology and Petroleum Engineering (University of Zagreb) to determine the mineralogy of limestones and the tephra layer. XRD patterns were taken using a Philips diffractometer (CuKα radiation, $U = 40$ kV, $I = 35$ mA) with graphite monochromator and proportional counter. For identification of non-carbonate components in limestones, two samples weighing up to 100 g were crushed to a size of 2–5 mm and digested in 5% acetic acid. The resultant patterns were recorded on untreated material as well as after glycerol and ethylene glycol treatment, and heating for 2 h at 600°C. To identify kaolinite, the X-ray pattern was recorded after the samples were boiled for 24 h in 18% HCl.

Five coal samples from seams from the middle and upper part of the section were selected for detailed analysis at the Department of Geological Sciences (University of Leoben). For microscopic investigations, the samples were crushed to a maximum size of 1 mm. Vitrinite reflectance was determined following standard techniques (Taylor et al. 1998). Maceral analysis was performed by a single-scan method (Taylor et al. 1998) with a Leica microscope using reflected white and fluorescent light. At least 300 points were counted. Huminite macerals were classified according to the nomenclature of Sýkorová et al. (2005). Maceral percentages were used to calculate facies indicators. The Tissue Preservation Index (TPI) and the Gelification Index (GI; Diessel 1986), modified for low-rank coals (Kalkreuth et al. 1991), are useful facies indicators (e.g. Bechtel et al. 2002, 2003, 2004); they were calculated for the Sinj samples according to the following formulas:

$$\mathrm{TPI} = \frac{\text{Textinite} + \text{texto-ulminite} + \text{eu-ulminite} + \text{corpohuminite} + \text{fusinite}}{\text{attrinite} + \text{densinite} + \text{macrinite}}$$

$$\mathrm{GI} = \frac{\text{Texto-ulminite} + \text{eu-ulminite} + \text{corpohuminite} + \text{densinite} + \text{macrinite}}{\text{textinite} + \text{attrinite} + \text{fusinite} + \text{inertodetrinite}}$$

The total carbon and total sulfur (S) contents were determined on a Leco elemental analyser. The total organic carbon content (TOC) was measured with the same instrument in samples pretreated with concentrated hydrochloric acid. Pyrolysis was carried out on the collected samples using a Rock-Eval instrument Version RE II+. This method normalises the amount of hydrocarbons (mgHC/g rock) and CO_2 released from kerogen during gradual heating in a helium stream to TOC to give the Hydrogen Index (HI) and the Oxygen Index (OI). As a pyrolysis maturation indicator, the temperature of maximum hydrocarbon generation (Tmax) was measured. Ash yield and moisture-content analyses followed standard procedures (Deutsches Institut für Normung 1978, 1980). All ash and sulphur values are given as weight percents on a dry basis (db).

The applied zonation of the lake environment largely follows Cohen (2003). The upper boundary of the profundal zone correlates with the upper boundary of the aphotic zone and the sublittoral zone has, in contrast to the littoral zone, no large submerged plants. Additionally to Cohen (2003), we distinguish the zone of seasonal lake-level fluctuation between the highest and the lowest water mark (*Damasonium* zone). The lake rim above the highest water mark, but occasionally influenced by waves, we refer to as the supralittoral zone.

Facies description and interpretation

The section was logged along a SW–NE striking gully W of the village Lučane in a small seasonal brook named Sutina. The gully cuts through a syncline structure, perpendicularly to its axis. The western wing of the syncline was measured and revealed a well-exposed, continuous section through a highly fossiliferous, coal-bearing upper part of the basin infill. The log is 137.5 m long (Fig. 3), starting 39.2 m below a 0.5-m-thick tephra horizon, ending 2.7 m above the base of the main coal layer. It bears large mammal remains documented in Olujić (1999) and Bernor et al. (2004) (GPS coordinates—base: N 43°43′13.9″ E 16°35′32.1″, top: N 43°43′10.9″ E 16°35′24.7″).

The succession consists of dominant limestones, coal seams, and several tephra beds (Fig. 3) and is subdivided into two limestone-coal cycles. Each

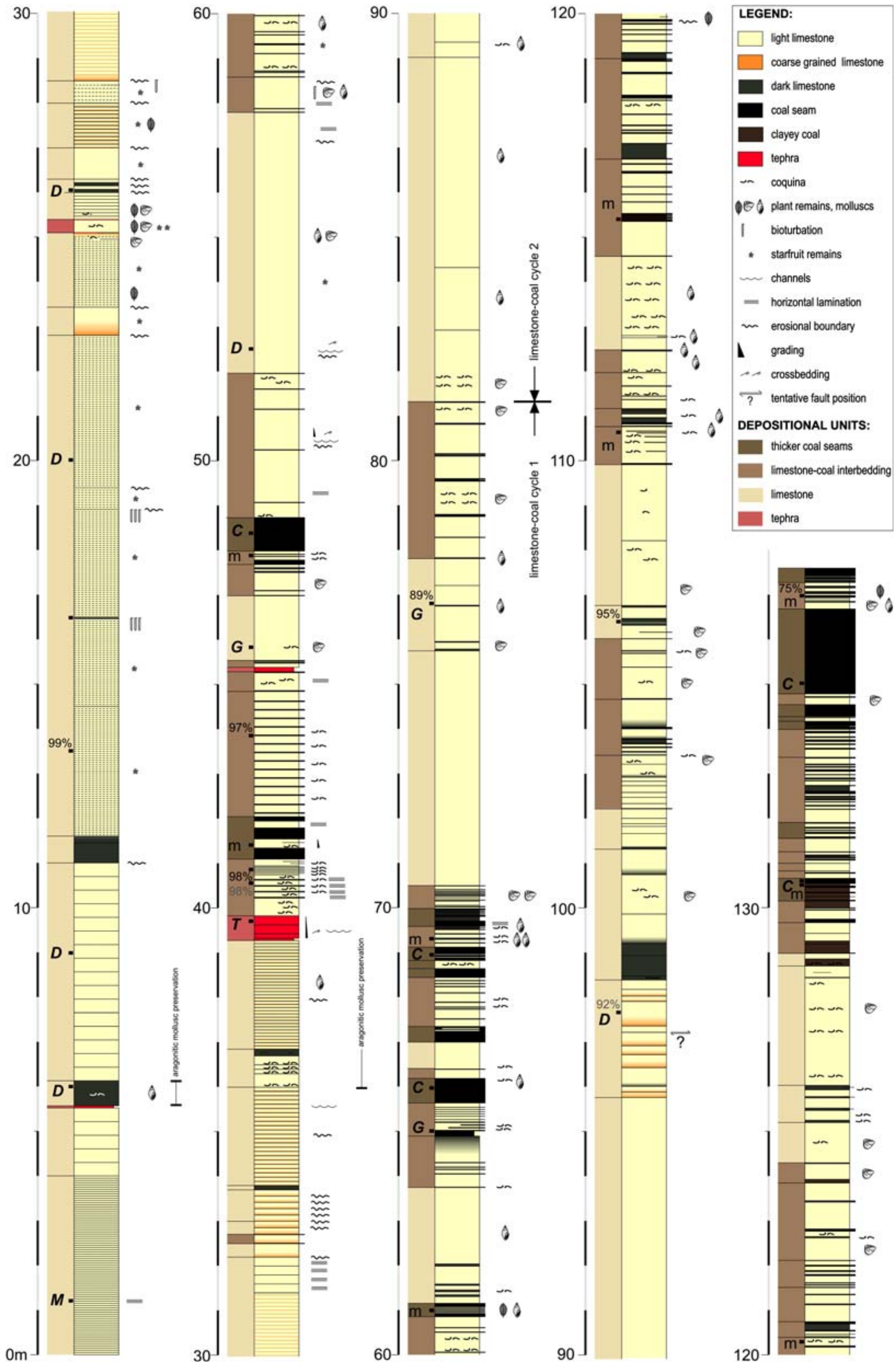
LEGEND:
light limestone
coarse grained limestone
dark limestone
coal seam
clayey coal
tephra
coquina
plant remains, molluscs
bioturbation
starfruit remains
channels
horizontal lamination
erosional boundary
grading
crossbedding
tentative fault position
DEPOSITIONAL UNITS:
thicker coal seams
limestone-coal interbedding
limestone
tephra
limestone-coal cycle 2
limestone-coal cycle 1
aragonitic mollusc preservation
0m
10
20
30
40
50
60
70
80
90
100
110
120
130
99%
97%
98%
89%
95%
92%
75%

◀ **Fig. 3** Section Lučane. Note the position of samples referred to in the text: D, *Damasonium* limestone; G, Gastropod wackestone and coquina; M, microbialite; C, coal; %, percentage of $CaCO_3$; m, mollusk bulk sample

cycle starts with fossil-poor, yellowish to light grayish, fine-grained limestone (0–25 m, 81–96 m), grading upwards into a fossil-rich transitional limestone facies of normal graded beds and organic-matter-enriched interlayers. The top of each cycle is formed by coal-bearing, highly fossiliferous units (40–81 m, 102–137 m).

The limestones are poor in fossils except for numerous minute molds and casts of *Damasonium sutinae* fruits. The mollusks are very scattered, mostly as molds. In contrast, the transitional facies and coal-seam-bearing intervals are highly fossiliferous. They contain species-poor but individual-rich lacustrine mollusk assemblages typically accumulated in coquinas.

The coal-bearing units comprise several coal layers, 1 cm–1.9 m thick, interbedding the carbonate sediment. Whereas the lower cycle includes six coaly intervals, only four intervals are present in the upper cycle. The presence of additional coaly intervals above the top of the section cannot be excluded. The distribution of seams thicker than 20 cm differs between the two cycles. Whereas relatively thick seams in cycle 2 are concentrated in its uppermost part, seams thicker than 20 cm occur in five coaly intervals distributed over about 30 m in limestone-coal cycle 1.

The limestones make up 89% of the studied succession. The $CaCO_3$ content is usually between 90 and 99%, and may be lower in limestones containing a higher proportion of organic matter. The main to exclusive carbonate mineral is calcite, while aragonite may locally attain 5 wt.%. The latter is related to the presence of gastropod shells.

Non-carbonate components in limestones consist of dominant amorphous organic matter (more than 50 wt.% of undissolved residium), and smaller amounts of terrigenous, mostly fine-grained siliciclastic material. The latter is represented by clay minerals including kaolinite, mixed layered clays, and probable smectite, chlorite, and vermiculite. Very rare silt-sized terrigenous particles are mainly represented by irregular to euhedral quartz, which may contain calcite inclusions. Rare zircon, tourmaline, tiny euhedral apatite, biotite, chlorite, amphyboles, and feldspars have also been identified. The zircon grains may be rounded or irregularly shaped. Rare rock fragments are quartz and chlorite aggregates. Some limestones contain authigenic pyrite framboids, which may attain 10 wt.%.

Four main limestone types are recognized: (1) *Damasonium* limestones, (2) Gastropod wackestone and coquinas, (3) Microbialites, and (4) "Massive limestones". *Damasonium* limestones are more common in the lower part of the succession than in its middle and upper parts. Gastropod wackestone and coquinas are common in the middle and upper horizons bounded to transitional and coal-bearing intervals of the succession. The other two facies apparently occur in all three parts of the succession.

Damasonium limestones

Description These limestones are massive, occasionally laminated, and commonly bioturbated. Their color may be either very pale orange (10 YR 8/2), or pale yellowish brown (10 YR 6/2) in limestones with more organic matter. The limestone textural types include mudstones, wackestones, and rare packstones. The matrix consists of micritic to microsparitic calcite with crystals up to 0.03 mm in diameter. Several types of silt-sized and larger calcite crystals are embedded in the matrix. They include (1) the trains of several calcite crystals, and individual calcites, both containing impurities, (2) the crystals with a zoned pattern and diameter up to 0.09 mm representing fish otoliths, (3) polyhedral to oval calcites and rhombic calcites, both about 0.04 mm in length, and (4) calcite rosettes.

Coalified plant debris and/or imprints of plant remains are common, as are encrusted fruits and stems. Vertical, narrow-winding traces probably represent the remains of macrophytes in living position, possibly roots. The fruits are slightly elongated, lensoid bodies, about 4 mm long, arranged in a star-like pattern of six follicles (Fig. 4a). They belong to the aquatic plant *D. sutinae* (Kerner 1905b). The encrustations consist of dentate, sparry calcite crystals. These calcites contain impurities, probably of organic matter. The plant encrustations may have helped prevent the later collapse of the plant and to preserve plant shape after its decay. This led to voids, which were later either filled with micritic calcite or left open, creating minute molds (Fig. 4b and c). Such molds represent the largest

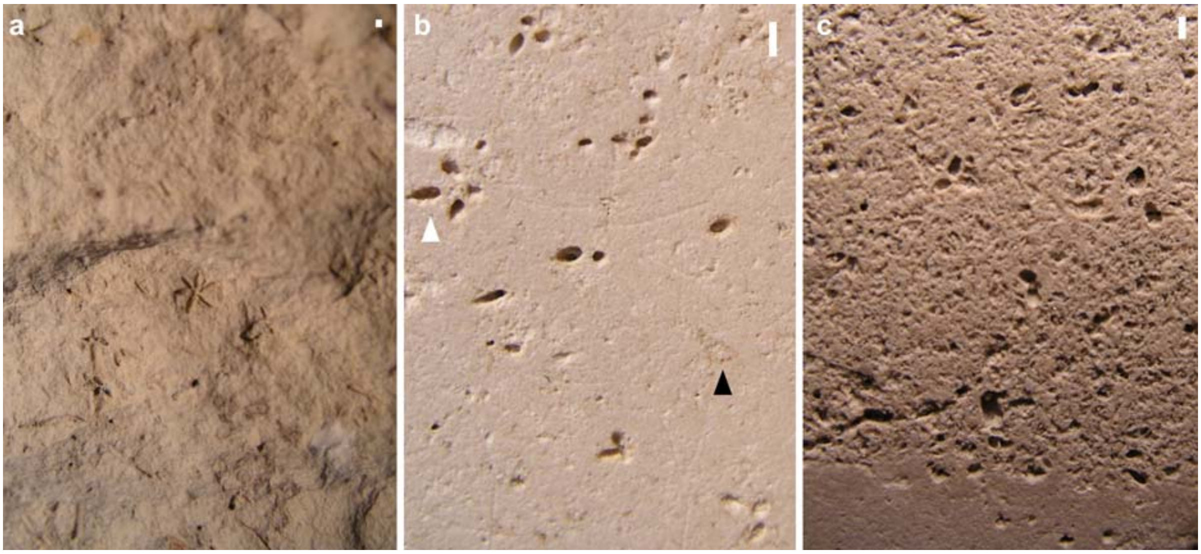

Fig. 4 *Damasonium* limestone facies: Lime wackestone with starfruit *Damasonium* sutinae fossil fruit remains. Sample position—20 m. Scale bars—1 mm. (**a**) Unpolished sample surface showing molds of star-shape arranged *D. sutinae* fruits. (**b**) Polished slab showing ellipsoidal to rounded sections of fruit molds (white arrow). The molds are surrounded by encrustation-walls clearly visible in fruit molds filled by micritic calcite after the plant material decayed (black arrow). (**c**) Polished slab showing resedimented limestone consisting of plant debris including *D. sutinae* fruits preserved as encrustation-walls surrounding infilled or empty molds. The accumulation is superposed to wackestone with scattered fruit remains

porosity type in the studied succession. The mudstones, wackestones, and packstones of *Damasonium* limestone facies mainly differ in the proportion of encrusted *Damasonium* fruits.

The *Damasonium* limestones also contain ostracods, bivalves, and gastropods with preserved or leached aragonitic shells. Filamentous microbial tufts attached to hard substrates such as bivalve shells or *Damasonium* fruits are also present. The rare, barely recognizable small micritic patches might represent remnants of microbial, micrite-calcified filaments. This limestone facies includes graded beds (Fig. 5) up to 15 cm thick, which show sharp, erosional bases. They range in character from coarse packstone to wackestone in the lower part, to wackestone containing finer particles at the top. The lower part of such beds is the coarsest sediment type of the studied succession; it represents an accumulation of stems, fruits of water plants, algal tufts, gastropods, ostracods, and bivalves. The relevant, graded interval of the bed may be overlain by horizontal laminae. Such graded beds are confined to transitional intervals preceding the coal-forming phases.

Interpretation Rooted aquatic macrophytes are restricted to the vegetated margins of carbonate, hard-water lakes, indicating deposition within a littoral, shallow-water environment (reviews in Tucker and Wright 1990; Platt and Wright 1991; Talbot and Allen 1996). *Damasonium sutinae* is very similar to the modern *Damasonium alisma* Miller, except for its size. Kerner (1905b) defines its size at 0.7–1.5 mm, with a largest measured seed of 4 mm. *Damasonium alisma* seeds are distinctly larger, attaining 5–14 mm in diameter (Stace 1997). *Damasonium alisma* thrives in ephemeral pools and ponds (at water depths to 50 cm) of the Mediterranean and NE Atlantic lowlands up to the latitude of SE England. It prefers poorly drained uppermost littoral mud-plains of lakes with seasonally fluctuating water level and flat bottom, or gently sloping pond margin morphology. The plant starts to grow only after the plain becomes flooded. Flowers and seeds then develop at the start of the dry season as the plain begins to dry. Once embedded in soft bottom sediment, the seeds can survive for years, waiting for the next flooding or other optimal environmental conditions (Wheeler 2007). They tolerate moderately acidic to alkaline freshwater, although they typically dominate in acid ponds because of low competitive pressure. The high predominance of *Damasonium*

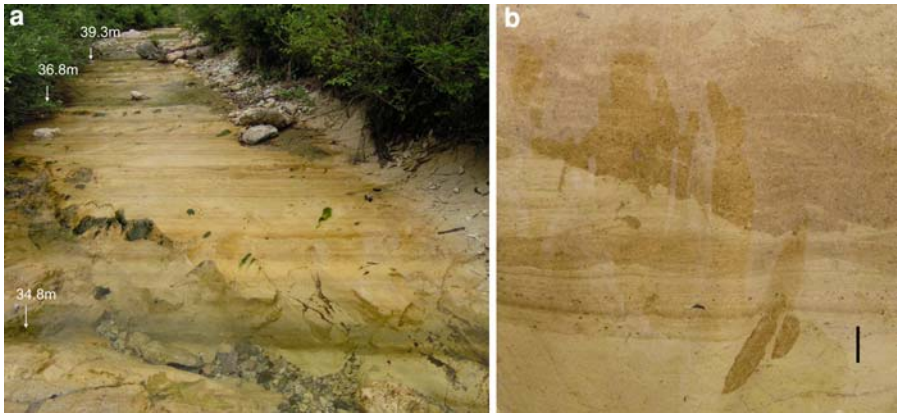

Fig. 5 *Damasonium* limestone facies: Transitional unit between the fossil-poor limestone and the limestone/coal interbedding. (**a**) Outcrop situation in front of the tephra layer showing graded limestones interrupted by two organic-rich dark limestone intercalations. (**b**) Detail photograph showing manifold current flow and organism-induced sedimentary structures with ripples, cross lamination, parallel lamination, graded bedding, erosional surfaces and bioturbations. Scale bar—1 cm

remains in some limestone intervals reflects the former presence of dense monospecific meadows. This corresponds to the modern, dense *Damasonium* monoculture, which strongly reduces the biodiversity of the lacustrine environment. The vegetated subaqueous environment also included a fish population, as indicated by fish remains.

Common plant encrustation reflects intense precipitation of carbonate from the lake water. This implies an important role of photosynthetic activity in the overall production of carbonate in this lake (Jones and Bowser 1978; Kelts and Hsü 1978; Monty and Mass 1979). The disintegration of encrustations yielded the encountered, isolated calcite crystals. Their derivation is indicated by the presence of organic matter impurities identical to impurity-bearing calcites found in original encrustations. Some of the calcite mud could have come from ancient carbonate rocks surrounding and underlying the lake. Moreover, calcite grains might have originated by heterogeneous nucleation, i.e. by growth of calcite over very fine calcite grains deriving from older carbonate sediments surrounding and underlying the lake, as in the case of the Plitvice Lakes (Srdoč et al. 1985). The process is probably enhanced by photosynthetic uptake of CO_2 (Stoffers 1975). Polyhedral to oval calcites, rhombic calcites, and calcite rosettes are authigene products, and represent features described from carbonate freshwater marsh sediments (Wright 1985). The occurrence of these grains points to temporary, short-lived changes to marsh environments, which presumably occupied neighboring, slightly shallower parts of the lake. The oval calcites might also have derived from the disintegration of characean gyrogonites. Characeans, however, which would have been expected to have thrived in the environment described above, have not been reliably identified.

Intercalations of erosionally-based, graded beds originated by infrequent, high-energy events, probably storm-induced processes. They caused erosion, resuspension of sediments, and deposition, including the concentration of the coarsest particles involved, and overlying fines. Irregular cross-laminae (Fig. 5b) might also be the product of storm-related events.

Gastropod wackestone and coquinas

Description The gastropod wackestone is characterized by indistinct lamination and by colors varying between yellowish gray (5Y 7/2) and pinkish gray (5YR 8/1). Very common plant stems and leaves occur parallel to bedding as imprints and coalified compressions. Also common are discontinuous laminae of organic matter and coal (Figs. 6 and 7). The coal also occurs in beds described separately below. Thin sections show poorly defined, brown to gray, diffusely bounded patches; they also show interspersed, thin, locally branching, crenulated stripes and lenses of dark brown, red or black organic matter (Fig. 6). The matrix of the limestones consists of micrite to sparite calcite grains up to 0.04 mm in

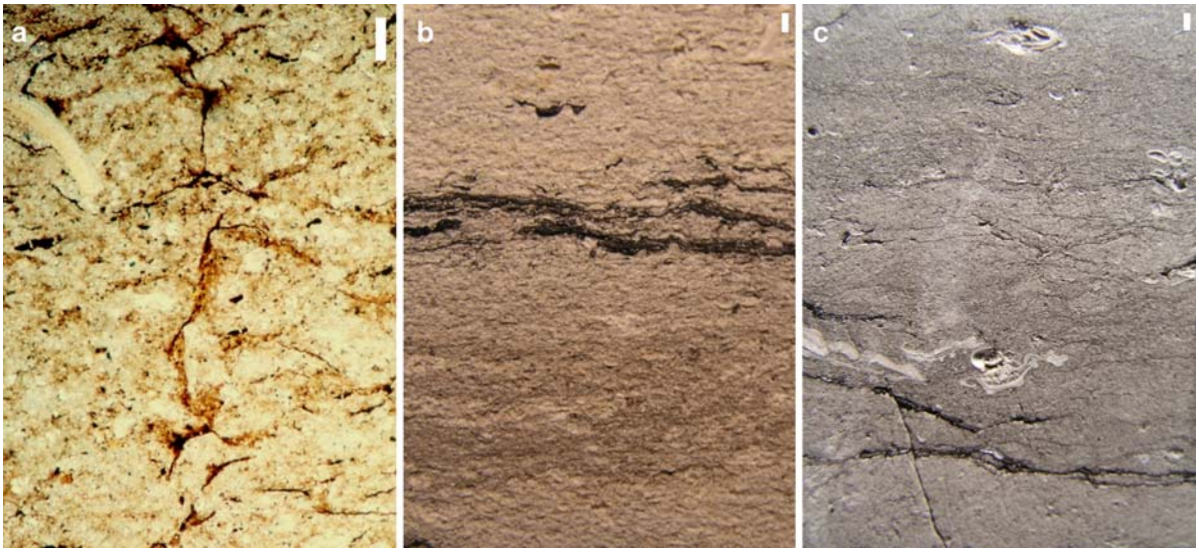

Fig. 6 Gastropod wackestone and coquina facies: (**a**) Photomicrograph of micritic to microsparitic limestone showing branching stripes of dark brown organic matter possibly representing carbonized plant roots. On the left is a fragment of aragonitic gastropod shell (light). Scale bar—100 μm. Sample position—76.8 m. (**b**) Laminated limestone with laminae of carbonized plant remains and coal. Scale bar—1 mm. Sample position—45.8 m. (**c**) Polished slab of gastropod-bearing laminated limestone rich in carbonized plant remains, partly crenulated. Dark brown organic material is interspersed in fine-grained limestone. Scale bar—1 mm. Sample position—76.8 m

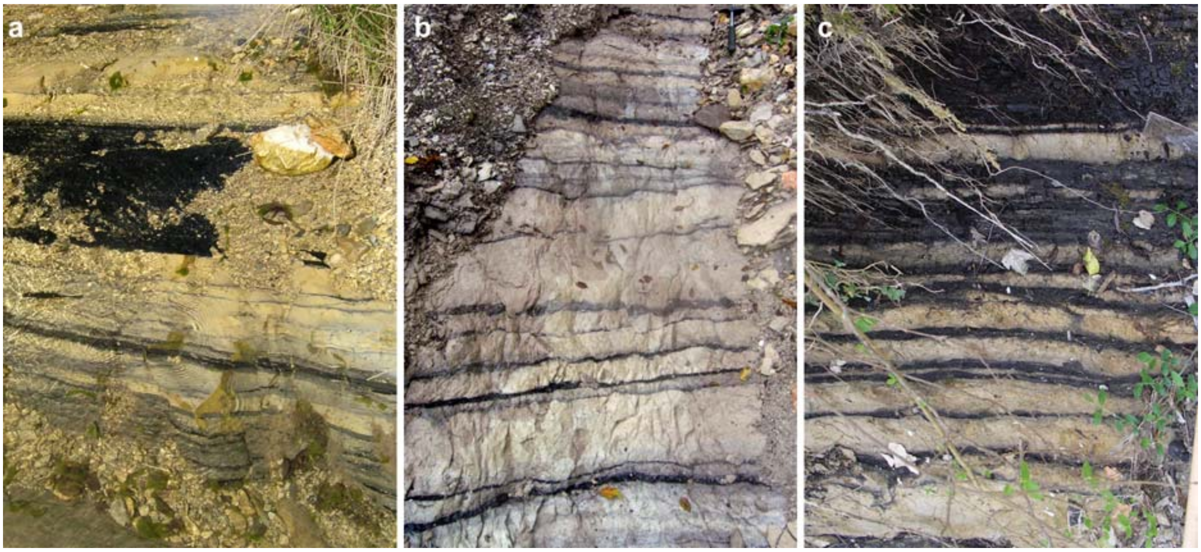

Fig. 7 Gastropod wackestone and coquina facies and coal facies: Limestone/coal interbedding. (**a**) Interbedding from the lower cycle including a 50-cm-thick coal bed at section position of 66 m (see also photomicrographs in Fig. 11a, b and d). (**b**) Interbedding from the upper cycle. Note the hammer for the scale at right upper corner of photograph. (**c**) Interbedding from the upper cycle directly underlying the main coal layer. The shown sequence is 110-cm-thick and ends with a 30-cm-thick coal seam from 134.4 m of the section

diameter. Several types of silt-sized and larger calcite crystals are the same as in the facies described above. Entire and fragmented aragonitic gastropod shells are common. In association with gastropods, there are recrystallized skeletons of bivalves, ostracods, fish otoliths, probable fish scales, plant encrustations, and tiny carbonized plant remains. Additional constituents of this facies are individual tufts, about 1 mm in diameter, of bundled microbial filaments with both the filament tubes and inter-tube areas cemented by sparry calcite. The tufts are attached to skeletal substrate.

Gastropod and bivalve shells, mostly non-fragmented, are locally packed, creating thin to 35-cm-thick coquina beds (Figs. 8 and 9). The coquina intercalations are commonly differentiated into gastropod- and into bivalve-dominated ones. The former are more frequently present in coal layers than the

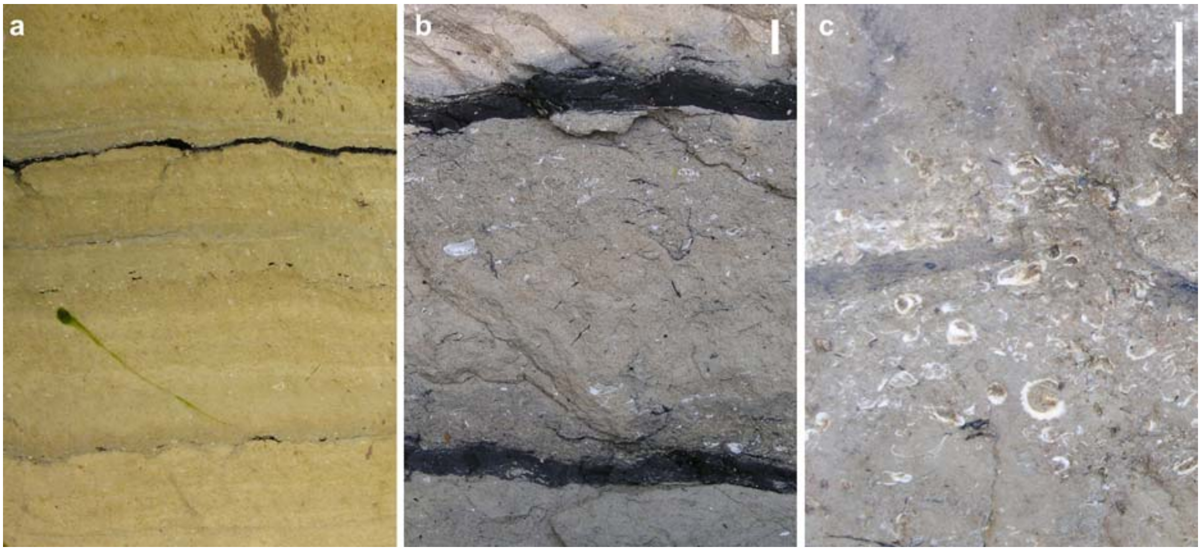

Fig. 8 Gastropod wackestone and coquina facies: Gastropod-dominated coquinas. (**a**) Coquina bearing varve-type laminated limestone from the lower cycle showing distinct and indistinct coal laminae. (**b**) Coquina between two thin coal seams. The shell accumulations are bounded to organic-matter-enriched portions, whereas the intercalated lighter limestone comprises only scattered shells. Scale bar—1 cm. (**c**) Gastropod coquina in an organic-matter-rich limestone. Scale bar—1 cm

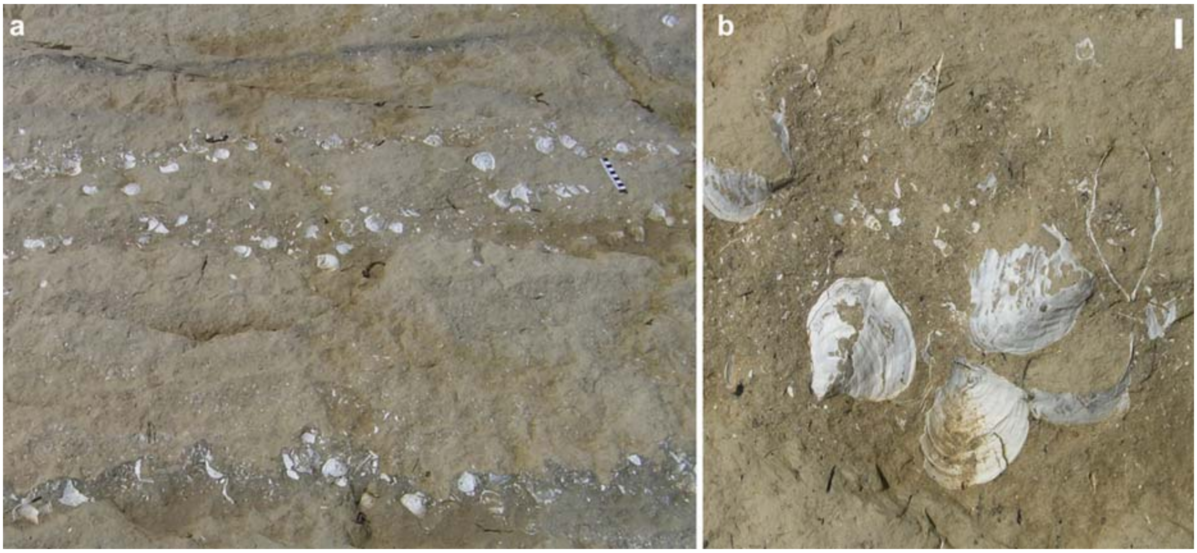

Fig. 9 Gastropod wackestone and coquina facies: dreissenid bivalve-dominated coquinas. (**a**) Three *Mytilopsis aletici*-dominated coquina beds. (**b**) Detail of the previous photograph. Scale bar—1 cm

latter. The color of the coquina is gray to brownish gray, locally dark gray due to the coaly matrix (Fig. 8b). The following species dominated in at least one of the samples: *Melanopsis lanzae* (Brusina 1874), *Melanopsis lyrata* (Neumayr 1869), *Prososthenia superstes* (Olujić 1999), *Prososthenia vojskavae* (Olujić 1999), *Theodoxus* (*Calvertia*) *imbricata* (Brusina 1878), *Theodoxus* (*Calvertia*) *lorkovici* (Brusina 1878), *Gyraulus* (*Gyraulus*) *geminus* (Brusina 1897), *Orygoceras dentaliforme* (Brusina 1882), *M. aletici* (Kochansky-Devidé and Slišković 1978), *Mytilopsis nitida* (Kochansky-Devidé and Slišković 1978), *Mytilopsis jadrovi* (Brusina 1892).

Interpretation The association of gastropods, bivalves, ostracods, microbial tufts, fragments of plant encrustations, and abundant, commonly coalified macrophyte remains in lime wackestone indicates restricted, calm, freshwater carbonate environments. Polyhedral to oval calcites, rhombic calcites, and calcite rosettes, also encountered in *Damasonium* Limestones, are typical authigenic products in marsh carbonates (Wright 1985). A similar indication is provided by tufts of microbial filaments, which resemble calcified heads built by *Scytonema*, described by Monty (1976) from the coastal freshwater marsh of Andros Island (Bahamas). Based on the fish remains, fishes represented a component of the ecosystem. As in the *Damasonium* limestones facies, the calcite crystals with organic impurities derived from the disintegration of plant encrustations. This points to submerged vegetation. Some of the polyhedral to oval calcites might have derived from the disintegration of characean gyrogonites.

The calcitic matrix, represented by irregularly distributed micrite, microsparite, and sparite, reflects diagenetic recrystallization processes. Framboidal pyrite indicates the presence of microbial processes in the sediment (Schieber 2002); these were related to the decaying organic matter, mainly represented by abundant plant remains. Vertical to sub-vertical, locally branching concentrations of organic matter possibly represent former rootlets, and the brown mottling might have resulted from initial pedogenic processes; the latter could have occurred either at very shallow depth or, possibly, during short-term exposure. The occurrence of coal and abundant plant remains in this facies represents a type of transition to the “pure” coal, as also suggested by the commonly encountered close association with coal seams.

The mollusk coquina intercalations in other limestone types originated, partly, by infrequent higher-energy events such as storms. Gastropod concentrations within the coal may have been produced by dead individuals floating into the mostly shallow, restricted bay environment (De Deckker 1988). An alternate explanation is an autochthonous origin due to the high reproduction rate of these animals (Talbot and Allen 1996). The gastropod assemblage, with dominating *Melanopsis*, *Prososthenia* and *Theodoxus*, indicates a littoral environment under fluvial influx. Today, *Melanopsis* and *Theodoxus* species prefer streams and estuarine lake habitats, respectively (Pfleger 1984). The extremely common hydrobiid *Prososthenia* preferred littoral mudplains, grazing there on algal mats (Quedens 1993; Rust 1997). In contrast, little is known about the ecology of the huge dreissenid bivalve *M. aletici*. This Dinaride Lake System endemic has a lucinoid shape unique for the dreissenids. Its monospecific accumulations are commonly represented by articulated shells oriented in the sediment parallel to the bedding. Like other dreissenid bivalves, it was possibly a filter feeder confined to sublittoral and littoral environments, up to the low-water-level mark. The large but circular and extremely thin-walled shell was perfectly adapted for mud reclining in calm-water environments. The minute, triangular *M. nitida* were attached to substrate, possibly to aquatic plants, by byssal threads.

The above discussion suggests calm, very shallow, freshwater settings dominated by carbonate marshes; these overlapped, in their distal part, with the vegetated shallow-water zone. Their proximal portions overlapped with peripheral swamps/mires.

Microbialites

Description This limestone is very pale orange (10 YR 8/2), faintly laminated, and bioturbated. Carbonized plant debris and impressions of plants are found on bedding planes and laminae. Diffuse lamination observed on the polished sections is hardly recognizable in thin section, which still shows an alternation of thin micritic laminae, and micrite to microsparite laminae containing calcite grains up to 20 µm in diameter. Both laminae types contain micrite-calcified microbial filaments about 0.02 mm in diameter. The filaments may be isolated, associated and oriented parallel to lamination or, rarely, in groups oriented perpendicularly to the lamination. The calcified filaments may be enveloped by radially-oriented calcite crystals. More and less distinct micrite spots probably originated through the breakdown of calcified, but non-cemented or partly cemented, meshes of microbial mats (Monty and Hardie 1976). Rare, scattered ostracods and recrystallized mollusk shells are also present. The lamination may locally be destroyed by bioturbation, resulting in sediment homogenization.

Interpretation The laminae consisting of microbial filaments are relics of former microbial mats. They may have thrived at different depths of the lake's photic zone (Talbot and Allen 1996). Together with vegetated environments, they probably occurred in the shallow parts of the lake. That is supported by the absence of subaerial exposure features and by common bioturbation, both suggesting shallow waters. The studied succession includes common laminated limestones without recognizable cyanobacterial filaments. They might still represent microbial laminites, but could also reflect a seasonally changing character of carbonate deposition without contribution of microbial organisms.

Massive limestones

Description Massive limestones alternate with other limestone facies and coal seams. They are mudstones, which may locally contain plant remains, very rare mollusks, and ostracods. Indistinct laminae and micrite spots occur occasionally. Bioturbation has also been observed. Some limestones lack clearly visible sedimentary structures and apparently represent originally different, but diagenetically altered facies.

Interpretation The limestones of this poorly defined facies might represent intensely bioturbated microbialites, or mudstones deposited in the deeper parts of the lake. The first interpretation seems more probable, at least for most of these limestones. This would agree with the locally occurring lamination and micrite spots, bioturbation features, and alternation of some of these limestones with coal seams inferred to have originated in marsh/swamps. In addition, the mudstone texture may have originated by transformation of partly calcified cyanobacterial mats into an amorphous, calcitic mud, as occurs in present-day freshwater marshes (Wright 1985). In general, the Massive Limestones may be tentatively interpreted as shallow-lake sediments.

Coal

Description The coal forms about 10% of the measured section and is mainly concentrated in its middle and upper part, representing the upper parts of the two limestone-coal cycles (Fig. 3). The coal laminae in the limestones mentioned above are accompanied by coal beds several centimeters to several decimeters thick (Fig. 7). Local residents reported that the exceptionally thick (1.9 m) coal seam was exploited by miners until the 1960s. Many abandoned mine facilities are still present near the studied outcrop. The contacts with neighboring limestones are either sharp or locally gradual. Seam thickness may change laterally. Some coal beds contain intercalated laminae and thin beds of the limestone described above. The coal and the limestones close to the coal may also contain the mollusk coquina intercalations described above and/or accumulations of aquatic plant stem crusts (Fig. 10). Vitrinite reflectance of two samples (0.37; 0.40%Rr) indicates a rank at the transition from lignite to subbituminous coal (*Mattbraunkohle* according to the German classification). This classification is also supported by TOC contents ($\sim$70%; dry, ash-free basis) and Tmax values (418–427°C; with the exception of MA68). Ash yield (20–30%) and sulphur content (6–9%) of the investigated coal samples are very high (Fig. 11). Inorganic carbon contents are generally low (<1%), although shells are visible in the sample from 130.6 m. The maceral composition and RockEval data of samples from the four lower seams are similar and differ from that of the 1.9-m-thick seam near the top of the studied succession (Fig. 11). The latter is therefore discussed separately.

The maceral composition in the four lower seams is dominated by huminite (82–88%). Liptinite (5.7–7.8%) and inertinite percentages (4–11%) are moderate. Within the huminite group, detrital macerals (detrohuminite) are significantly more abundant (70–73%) than preserved tissues (telohuminite: 9–15%), and gelified huminite macerals predominate over

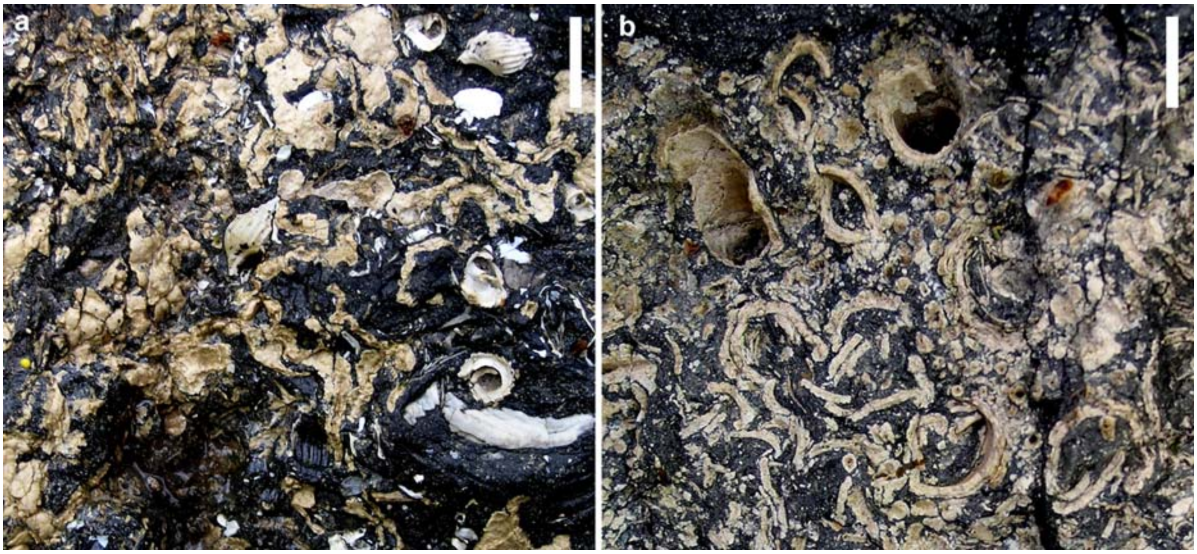

Fig. 10 Coal facies: Pseudocoquina consisting of fragmented and whole encrusting walls of aquatic plant stems in a coal matrix. Section position—137 m, scale bar—1 cm. (**a**) Including well-preserved, ribbed melanopsid gastropods. (**b**) In addition to the crushed crusts, the whole ones missing the decayed stem are visible in the upper part of the photograph

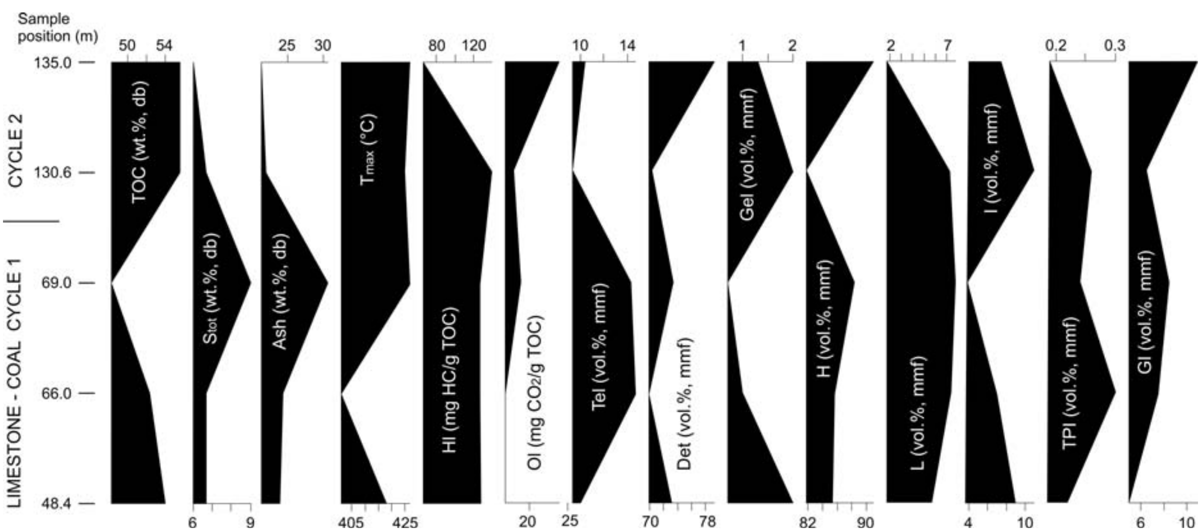

Fig. 11 Coal facies: Position, ash yield, total sulfur and organic carbon contents, Rock Eval parameters, maceral composition, and facies indicators for analyzed samples. TOC = Total organic carbon; S_{tot} = Total sulphur content; T_{max} = Temperature of maximum pyrolysis yield; HI = Hydrogen Index; OI = Oxygen Index; Tel = Humotelinite; Det = Humodetrinite; Gel = Humocollinite; H = Sum of Huminite; L = Sum of Liptinite; I = Sum of Inertinite; TPI = Tissue Preservation Index; GI = Gelification Index; db = Dry basis; mmf = Mineral matter-free basis

ungelified macerals (Fig. 12). This yields low TPI (0.2–0.3) and high GI values (5–9). Alginite (up to 2.4%) occurs in all samples along with terrestrial liptinite (cutinite, fluorinite, sporinite) and liptodetrinite. Percentages of leaf-derived macerals (phyllohuminite + cutinite + fluorinite; Fig. 12a, b) range from 5 to 6%. (Semi-)pyrofusinite and inertodetrinite are the main inertinite macerals. Funginite is abundant as well (up to 2%; Fig. 12c). HI (127–139 mgHC/gTOC), and OI values (17–19 $mgCO_2$/gTOC) vary within a narrow range (Fig. 11). Coal from the uppermost seam differs from other coal

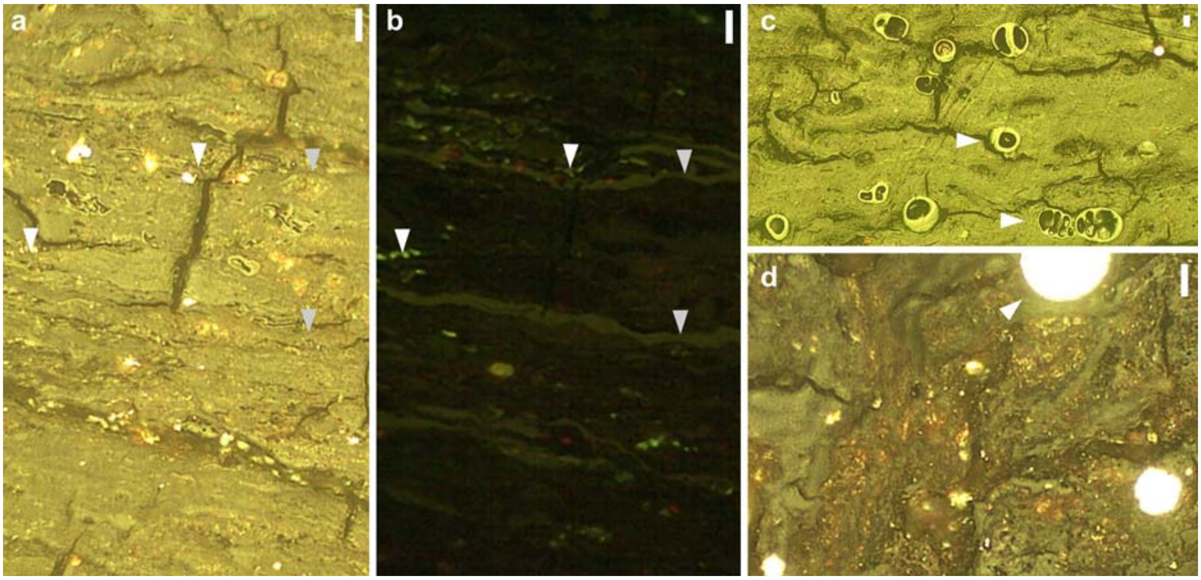

Fig. 12 Coal facies: photomicrographs. Scale bar—10 µm. (**a**) Strongly gelified detrital coal with cutinite (gray arrows) and fluorinite (white arrows). Incident white light, sample position—66 m. (**b**) Same field as (**a**) but under blue-light irradiation. (**c**) Abundant funginite (arrow) in strongly gelified detrital coal. Sample position—48.5 m. (**d**) Ash-rich coal. Sample position—66 m

samples in having a significantly lower liptinite content (1.7%), slightly higher huminite content (91%), lower percentage of leaf-derived macerals (1.4%), and an apparent absence of alginite. However, TPI (0.2) and GI values (11) are in a similar range (Fig. 11). A relatively low HI value (66 mgHC/gTOC) reflects the low liptinite content.

Interpretation The coals alternating with limestones document temporary swamp/mire formation in which abundant plant material accumulated, but was not oxidized. These environments may have been generated by the shallowing of the carbonate lake, enabling their progradation over the carbonate environments. The importance of numerous lignite intercalations in the succession is discussed below. High ash yields prove the formation of the studied seams in frequently flooded low-lying mires. The presence of alginite shows at least temporary subaquatic conditions during deposition of the lower four seams. Abundant leaf-derived macerals are typical for subaquatic environments. A lower percentage of alginite and leaf-derived macerals indicates that subaquatic conditions did not prevail during deposition of the uppermost seam.

High sulphur contents in all seams are typical for calcium-rich swamps and argue for high bacterial activity promoted by neutral to alkaline conditions (e.g. Petrascheck 1952; Taylor et al. 1998). Bacterial activity not only yields high sulphur contents, but also decomposes plant material. Therefore, the high GI and the low TPI support the above interpretations of pH values. Moreover, the low TPI values suggest that plants with a low decay-resistance (e.g. angiosperms) contributed more to the biomass than decay-resistant plants (e.g. gymnosperms). Bacterial biomass incorporated into the peat substance can increase the hydrogen content (and the hydrogen index) of coal. The observed relatively low HI values (66–139 mgHC/gTOC) show that such an incorporation was not very important for the Sinj Basin coal production. In contrast, the likely carbonate-rich "karst" coal from the late Cretaceous/early Paleocene of central Istria (Hamrla 1959) has much higher HI values (up to 330 mgHC/gTOC; Rainer 2003).

Clay (Tephra)

Description There are 5 clay intercalations in limestones traced at 5.5, 25.1, 25.4, 39.3 and 45.3 m of the section (Fig. 3). They are sharply bounded and light grey, dark brownish and dark green (Fig. 13). The brown clays at 25.1 m and at 25.4 m are only

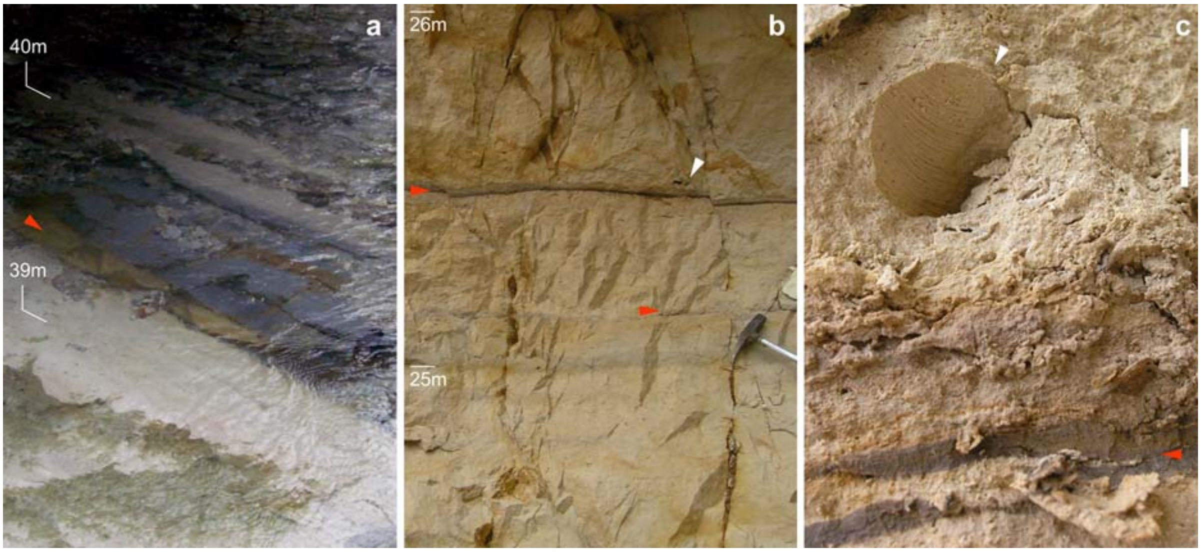

Fig. 13 Tephra facies: (**a**) Thick pyroclastic layer starting at 39.3 m of the section with the tephra clay (red arrow) followed by ripple and crossbedded, dark, pyroclastic, mineral-rich sediment. (**b**) Thin dark clay intercalated into light limestone rich in plant remains. Lower red arrow: a second indistinct clay lamina. White arrow: a shell magnified in the following photograph. (**c**) Detail of the previous photograph showing the clay layer and the exterior imprint of a unionid bivalve shell. Scale bar—1 cm

1 cm thick—the intercalation at 25.1 m disappears laterally (Fig. 13b and c). Others are between 10 and 5 cm thick. The sample from 39.3 m (Fig. 13a) is a vitroclastic tuff mainly consisting of subparallel, elongated, 0.04- to 0.06-mm-long glass particles. The proportion of the crystalloclasts is <5%. Visually recognizable are biotite, quartz, chlorite, very small apatite crystals, and probable amphibole. Brown patches probably represent devitrification products. The X-ray diffraction pattern indicates more than 70 wt.% of amorphous components and smectite (and probable mixed-layer clay mineral), both of which are products of devitrification, 5 or less weight percent biotite, 5% plagioclase and traces of K-feldspars, and more than 5% quartz. The X-ray analysis also revealed gypsum, which is probably an authigene constituent.

Interpretation Microscopic and chemical analyses suggested an andesite-dacite character of the volcanic activity. Consequently, the tephra compositions correspond well with a series of similar volcanic ash layers of the Sinj Basin described in detail by Šušnjara and Šćavničar (1974). The absence of terrigenous components, and the small dimensions of particles in the tephras, suggests a pyroclastic fall of volcanic ash derived from distant eruptions, perhaps in Bosnia and Herzegovina (Šušnjara and Šćavničar 1974). On the other hand, they could be contemporaneous to strong Miocene volcanic activity in the southern Pannonian Basin System, resulting from the climax of its syn-rift phase (Pamić et al. 1995; Pavelić 2001).

Discussion

Based on the above features and interpretations, the overall picture of the younger period of the Lake Sinj includes sublittoral, littoral, and supralittoral environments of a dominantly hard-water lake. The lake was probably perennial, as there are no reliable indications of subaerial exposure.

Acidification events

The deposition of the *Damasonium* Limestone, however, was probably accompanied by periodic changes of water level, triggering the massive production of fruit remains. The fruits were transported down to the sublittoral zone by wind or water, for example during occasional storm events. Their accumulations together with prososthenian snails in the graded beds of the transitional zone point to reworking and lake bottom-sediment redeposition during such events. The two transitional zones may represent the environmental transition from the littoral into the infralittoral zone. Moreover, the fossil scarceness, poor content of organic matter, and leaching of aragonitic mollusk shells within the *Damasonium* limestones indicate acidification of the lacustrine environment. This would have promoted monoculture starfruit meadows within the uppermost littoral rim of the lake. With the transitional zone and the coal/limestone interbedding, the situation changes: lake biodiversity rapidly increases. Hence, masses of mollusks and rich organic matter production come to characterize the ecosystem. The high organism diversity is, in contrast to acid lakes and ponds, a typical feature of alkaline lakes (Brönmark and Hansson 2005).

The acidification hypothesis does not fit with the presence of intensive carbonate production, which clearly points to a hard-water lacustrine depositional environment. Hard-water lakes are always base-enriched. Yet the high production of *Damasonium* fruits points, as discussed above, to seasonal aerial exposure and drying of the lake's uppermost littoral zone. During low stands, the lime mud—originally representing the anoxic environment—becomes aerated and oxidized, triggering the release of H^+ ions. When lake levels rise and that sediment becomes flooded, pH may decrease with catastrophic effects on organisms (Brönmark and Hansson 2005). Brief, periodic acidification events impact the equilibrium and prevent ecosystem diversification. Such related oxidation processes could also explain the unexpectedly low organic content and the light color of apparently well-aerated muddy sediment. The intensive bedding (beds of 5–30 cm) in the lower part of the section probably reflect reduced carbonate production due to short-term acidification events.

Hard-water lake carbonate production

Physical structures and biological criteria indicate a low-gradient ramp margin of the lake, which was of a low-energy type. The high-energy events were restricted to reworking of mud and biogenic carbonate particles by rare storms. The lake occurred under a wet, subtropical climate based on palynology, which indicates swamp and terrestrial vegetation (Šušnjara and Sakač 1988). This and other studied parts of the lake history are highly dominated by lacustrine limestones, suggesting a long-lived, stable depositional setting within the basin (Šušnjara and Sakač 1988). The common occurrence of plant and cyanobacterial filament encrustations, and of calcite grains identified as their disintegration products, document the inorganic precipitation of carbonate from the lake water. The precipitation of calcite in hard-water lakes is largely related to photosynthetic activity in the water and contributes considerably to carbonate sediment (reviews in Tucker and Wright 1990; Platt and Wright 1991; Talbot and Allen 1996). This process was apparently also important in Lake Sinj. Accordingly, both the calcite encrustations and most of the calcitic mud represent direct precipitates. Some of the calcite mud may have resulted from the breakdown of encrustations. The biogenically-induced precipitation therefore represents the most important contribution to the carbonate sediment accumulation in Lake Sinj. Minor contributions of carbonate material derive from mollusks and ostracods.

The input of fine-grained siliciclastic material was volumetrically insignificant and restricted to silt-sized particles scattered in limestones. It might have reached the lake by winds or by spreading overflows. Quartz grains with calcite inclusions originate by authigenesis in limestones; most of these grains therefore probably derived from older limestones in the vicinity. To a lesser degree, such grains might have been recycled from sandstones. The euhedral apatite, biotite, and some quartz shards derived from volcaniclastic deposits as ultimate sources. Ultimate sources for the subrounded zircon, quartz, tourmaline, rounded chlorite, and rock fragments were mainly older clastic rocks. As both these particle groups have been identified in a variety of the Dinaric limestones (Crnjaković 1994), they stem at least in part from the lake's carbonate catchment area.

Depositional environments and sedimentary evolution

The features of the facies suggest that Lake Sinj environments included vegetated areas dominated by submerged plants, areas covered by cyanobacterial mats, carbonate marshes, and peripheral swamps/mires. Previous workers already identified submerged lake and marsh/swamp plants, but also land plants indicating forests, which surrounded the lake (Kerner 1905b, 1916a, b; Žagar-Sakač and Sakač 1987; Šušnjara and Sakač 1988). The depth difference between swamp/marsh environments responsible for the origin of coal, and those related to the limestones, were probably rather small, based on the inferred, predominantly shallow environments for the limestones. Accordingly, the lake-level fluctuations were probably modest. Moreover, the relative lake level was rather stable during the comparatively long period studied here.

We tentatively recognize two types of sedimentary evolution within the basin fill, both corresponding to the shallow freshwater realm. The first one reflects rather stable conditions and is characterized by relatively uniform limestone deposition; it commonly comprises remains of submerged vegetation and perhaps microbial mats. The second type was comparatively shallower on average and environmentally more variable/unstable. Here, the shoal and/or very shallow bay with thriving herbs, reeds, mollusks, and cyanobacteria mats alternated periodically with restricted peripheral swamps/mires accumulating abundant plant material. The lower part of the studied succession lacking coal seams (Fig. 3) probably originated mostly within the first, relatively stable sector. In contrast, the middle and upper parts of the succession, characterized by alternating limestone and coal, reflect alternating conditions related to environmental instability of marginal to peripheral lacustrine areas.

Orbitally-forced depositional cycles

The succession comprises two large-scale cycles of environmental change. These start with organic-matter-poor limestones, pass through a transitional zone of graded and/or organic-matter-enriched limestones, and end at the coal-seam-bearing limestones and coals. Those latter coal-building phases are subdivided into smaller cycles of organic matter enrichment, with three outcropped intensity maxima of coal seam building—two for the lower and one for the upper phase (Fig. 3). The apparent relation of those periodic and cyclic environmental perturbations to orbitally-forced climatic changes was discussed in a report by Mandic et al. (2006).

The studied coal seams represent textbook examples for coal formation in alkaline environments. Typical features include high sulphur contents, poor tissue preservation, and strong gelification of plant material (e.g. Taylor et al. 1998). All these characteristics are mainly controlled by hard water, which buffers the organic acids formed during peatification. Therefore, mires formed in carbonate lakes are characterized by high pH values, which promote bacterial activity. Whereas some coals formed in carbonate-rich environments are rich in hydrogen (e.g. coal from Istria; Hamrla 1959), this is not the case in the Sinj Basin.

The above processes might have taken place under open lake conditions with a comparatively stable lake level, low runoff rate, and a very low input of eroded detritus. Such conditions characterize areas dominated by carbonate bedrock geology, as in Lake Sinj. Alternatively, Lake Sinj might have been hydrologically closed, with the character of the runoff and detritus supply as above; the lake level might have been quasi-stable and related to the karst groundwater level. In both cases, minor lake-level fluctuations due to orbitally-induced, climatically-controlled fluctuations in precipitation rate could have influenced the marginal lake environments and produced limestone/coal cycles.

A detailed palynological and cyclostratigraphic analysis from the Pliocene of the Ptolemais Basin (northern Greece) indicated coal production is generally associated with dry-climate phases, whereas the carbonate-rich intervals reflect humid phases (Kloosterboer-van Hoeve et al. 2006).

Mollusk response to environmental change

The mollusks imply fluvial input throughout the section. The gastropods indicating such inflow are conspicuously common in coal- and organic-matter-rich intervals. Hence during the organic matter accumulation and the coal-building phases, small freshwater streams still influenced the marginal lake environment, but lake level still fell due to the dry climate phase. The large dreissenid bivalves preferred the intercalated limestones, i.e. deeper littoral environment established within the humid-climate phases.

The distribution of hydrobiid (*Prososthenia*) and melanpsid gastropod species corresponds with the evolutionary scheme presented earlier by Olujić

(1936, 1999). Hence their phylogenetic lines show, around two coal-seam-bearing horizons, smooth morphologies and low morphologic disparity/taxonomic diversity. The radiation pulse started above the top of the first transgressive-regressive cycle. The diversification enriched the fossil record from 5 to 14 subspecies-level taxa, characterized by prominent sculptural elements. The massive extinction event around the top of the second cycle diminished the species richness to the starting position, although with completely renewed taxonomic content.

Marginal environments of Lake Sinj and its pull-apart tectonic setting

Lateral to the studied section, small lenses with fluvial conglomerates composed of carbonate pebbles are intercalated into the coal/limestone succession. This indicates the fluvial input predicted by mollusk composition. They occur in the southern wing of the syncline, about 250 m SW from the top of the section (cf. Olujić 1999).

The up to 2-m-thick megabreccia beds intercalated there (Fig. 14) indicate the steep original margin of the basin. The combination of flat lake bottom and steep margin morphology fits well with the tectonic background of the basin, which is interpreted as a pull-apart structure (cf. Tari 2002).

Fig. 14 Two breccia and conglomerate lenses intercalated into the limestone/coal interbedding of the southern anticline wing located about 250 m SSE from the top of the studied section

The relatively slow subsidence rate of that pull-apart basin can be explained by the extended diapirism within the basinal basement. The Permo-Triassic evaporites cropping out today in the north-western part of the basin show an erosive discordant contact to the basal Lake Sinj deposits and were apparently present there since the initial Miocene basinal flooding (Šušnjara and Sakač 1988, Fig. 2).

Conclusions

The studied Miocene lacustrine carbonates of the Sinj Basin originated in the early Middle Miocene during the late evolutionary stage of perennial, long-lived Lake Sinj. This was a shallow, calm, mainly hard-water lake throughout the studied time interval. The reevaluation of earlier data confirms that this applies to its entire evolution. The lake was situated within a carbonate area, and the supply of siliciclastic detritus to the lake was negligible. The biogenically-induced precipitation is the key contribution to the carbonate sediment accumulation in Lake Sinj. Minor contributions of carbonate material derive from mollusks and ostracods.

Long-lived Lake Sinj was characterized by low-gradient, low-energy margins. In contrast, the hinterland margin was steep, probably induced by a deep horizontal fault zone. Such morphology is congruent with the predicted pull-apart tectonic background of the basin.

The ecosystem comprised a variety of environments including (1) sublittoral or the photic zone below the fair weather wave base, (2) lower littoral or the photic zone above the fair weather wave base, (3) upper littoral with vegetated areas dominated by aquatic, perennial plants, (4) *Damasonium* zone corresponding to the uppermost littoral area between the highest and the lowest water mark inhabited by starfruit meadows, (5) areas covered by cyanobacterial mats, (6) carbonate marshes, (7) peripheral swamps, (8) stream catchment areas, (9) frequently flooded low-lying mires and (10) high-lying dry mires, the later inhabited by large land mammals related to elephants and rhinoceroses.

We recognize two types of sedimentary evolution, both related to the lake's photic zone. The first resulted from deposition within rather stable sublittoral and littoral conditions. It was characterized by relatively uniform deposition of bedded limestones. That depositional phase was characterized by abundant starfruit remains and otherwise remarkably low biotic diversity. These features were interpreted to reflect periodic acidification events caused by recurring flooding of adjoining starfruit meadows due to climate-driven lake-level fluctuations. The second type of sedimentary evolution resulted from deposition in the shallow littoral zone. The changing water-level conditions resulted in alternating limestone/coal seam production. That alternation was triggered by the short-term, orbitally-forced cyclic fluctuation of humid and dry periods.

The documented paleoenvironmental evolution marks the end of the long-lived Lake Sinj. Its final disintegration therefore went through two superposed, large-scale, shallowing upward depositional cycles. Each of them started with a series of organic-matter-poor limestones, then passing through tempestite series, ending in the coal/limestone interbedding series; the latter was subdivided into several subcycles of organic matter enrichment. Whereas the shallowest part of the first cycle is still in the temporarily flooded lower mire facies, the upper cycle marks, at least temporarily for the first time within the section, the complete drying of the environment (based on the presence of the high mire).

Acknowledgments Our sincere thanks for support and help with the investigation go to Jeronim Bulić, Zlata Jurišić-Polšak, Jakov Radovčić (all Croatian Natural History Museum, Zagreb), Raymond Bernor (Howard University, Washington, US), and Arjan de Leeuw (Utrecht University). We are indebted to Franz Topka (NHM, Vienna) and Felix Marx (Univ. Bristol) for assistance with the field and the laboratory work. The study was funded by the Austrian FWF Project P18519-B17: "Mollusk Evolution of the Neogene Dinaride Lake System" and by the Republic of Croatia, Ministry of Science, Education and Sports Projects: "Neogene terrestrial environments of the Pannonian Basin and karst region" no. 195-1951293-2703, and "Evolutionary changes of the Dinarides from subduction to modern Adriatic beaches" no. 119-1191155-1159.

References

Anadon P, Cabrera LI, Kelts K (1991) Lacustrine facies analysis. Blackwell Scientific Publications, Oxford

Bechtel A, Sachsenhofer RF, Kolcon I, Gratzer R, Otto A, Püttmann W (2002) Organic geochemistry of the Lower Miocene Oberdorf lignite (Styrian Basin, Austria): its relation to petrography, palynology and the paleoenvironment. Int J Coal Geol 51:31–57

Bechtel A, Gruber W, Sachsenhofer RF, Gratzer R, Lücke A, Püttmann W (2003) Depositional environment of the Late Miocene Hausruck lignite (Alpine Foreland Basin): insights from petrography, organic geochemistry, and stable carbon isotopes. Int J Coal Geol 53:153–180

Bechtel A, Markic M, Sachsenhofer RF, Jelen B, Gratzer R, Lücke A, Püttmann W (2004) Paleoenvironment of the upper Oligocene Trbovlje coal seam (Slovenia). Int J Coal Geol 57:23–48

Bernor RL, Bi S, Radovčić J (2004) A contribution to the evolutionary biology of Conohyus *Olujici* n.sp. (Mammalia, Suidae, Tetraconodontinae) from the early Miocene of Lučane, Croatia. Geodiversitas 26:509–533

Brönmark C, Hansson LA (2005) The biology of lakes and ponds, 2nd edn. Oxford University Press, New York, USA

Brusina S (1874) Fossile Binnen-Mollusken aus Dalmatien, Kroatien und Slavonien nebst einem Anhange. Actienbuchdruckerei, Agram

Brusina S (1878) Molluscorum fossilium species novae et emendatae, in tellure tertiaria Dalmatiae, Croatiae et Slavoniae inventae. J Conchol 1878:1–10

Brusina S (1882) *Orygoceras* eine neue Gasteropodengattung der Melanopsiden-Mergel Dalmatiens. Beitr Palaeontol Oesterr-Ung Orient 2:33–46

Brusina S (1892) Fauna fossile terziaria di Markuševec in Croazia. Con un elenco delle Dreissensidae della Dalmazia, Croazia e Slavonia. Glasn Hrv Naravosl Dr 7:113–210

Brusina S (1897) Gragja za neogensku malakološku faunu Dalmacije, Hrvatske i Slavonije uz neke vrste iz Bosne i Hercegovine i Srbije. Djela Jugosl Akad Znan Umjetn 18:1–43

Bulić J (1999) Olujić i geologija. Komentar uz tablicu s razvojnim nizovima fosilnih puževa iz neogenskih naslaga okolice Sinja. In: Jurišić-Polšak Z (ed) Josip Olujić. O razvojnim nizovima nekoliko melanopsida i prozostenida iz sarmatskih naslaga okolice Sinja (Dalmacija, Hrvatska). Hrvatski prirodoslovni muzej, Zagreb and Provincijalat Franjevačke provincije presvetog Otkupitelja, Sinj, pp 113–126

Bužek Č (1982) Ceratostratiotes Gregor, an extinct water plant of uncertain affinity from the European Miocene. Vestn Ustred Ust Geol 57:285–294

Cohen AC (2003) Paleolimnology. The history and evolution of lake systems. Oxford University Press, New York

Crnjaković M (1994) The detrital versus authigenic origin and provenance of mineral particles in Mezozoic carbonates of central Croatia karst area. Geol Croat 42:167–179

De Deckker P (1988) Biological and sedimentary facies of Australian salt lakes. Palaeogeogr Palaeoclimatol Palaeoecol 62:237–270

Deutsches Institut für Normung (1978) Feste Brennstoffe. Bestimmung des Wassergehaltes. DIN 51718

Deutsches Institut für Normung (1980) Feste Brennstoffe. Bestimmung des Aschegehaltes. DIN 51719

Diessel CFK (1986) On the correlation between coal facies and depositional environments. Proc 20th Symp Dep Geol, Univ. Newcastle, N.S.W., pp 19–22

Goddard EN, Trask P, De Ford RK, Rove ON, Singewald JT Jr, Oberbach RM (1963) Rock-Color chart. Geological Society of America, New York

Hamrla M (1959) On the conditions of origin of the coal beds in the Karst region. Geol (Ljub) 5:180–264

Harzhauser M, Mandic O (2008a) Neogene Dreissenids in Central Europe—exploring the limits. In: Van der Velde G, Rajagopal S, Bij de Vaat A (eds) Zebra mussels in Europe (in press)

Harzhauser M, Mandic O (2008b) Neogene Lake Systems of Central Europe—diversities, gradients and faunistic interrelations. Palaeogeogr Palaeoclimatol Palaeoecol 260:417–434

Jones BF, Bowser CJ (1978) The mineralogy and related chemistry of lake sediments. In: Lerman A (ed) Lakes, chemistry geology physics. Springer-Verlag, New York, pp 179–235

Jurišić-Polšak Z (1999) O Olujićevu dosada neobjavljenom radu. In: Jurišić-Polšak Z (ed) Josip Olujić. O razvojnim nizovima nekoliko melanopsida i prozostenida iz sarmatskih naslaga okolice Sinja (Dalmacija, Hrvatska). Hrvatski prirodoslovni muzej, Zagreb and Provincijalat Franjevačke provincije presvetog Otkupitelja, Sinj, pp 89–112

Jurišić-Polšak Z, Bulić J (2007) Pradavno Paško jezero. Hrvatski prirodoslovni muzej, Zagreb

Kalkreuth W, Kotis T, Papanicolaou C, Kokkinakis P (1991) The geology and coal petrology of a Miocene lignite profile at Meliadi Mine Katerini, Greece. Int J Coal Geol 17:51–67

Kelts K, Hsü KJ (1978) Freshwater carbonate sedimentation. In: Lerman A (ed) Lakes, chemistry, geology, physics. Springer-Verlag, New York, pp 295–323

Kerner F (1905a) Gliederung der Sinjaner Neogen-formation. Verh Geol RA 1905(6):127–165

Kerner F (1905b) Neogenpflanzen vom Nordrande des Sinjsko polje in Mitteldalmatien. Jahrb Geol RA 55:593–612

Kerner F (1916a) Alt- und jungtertiäre Pflanzenreste aus dem obersten Cetinatale. Verh Geol RA 1916(8):180–191

Kerner F (1916b) Erläuterungen zur Geologischen Karte der Österr.- Ungarn. Monarchie 1:75.000, Sinj und Spalato. Geologische Reichsanstalt, Wien

Kerner F (1916c) Sinj und Spalato 1:75.000/neu aufgenommen und bearbeitet in den Jahren 1902–1909. Geologische Reichsanstalt, Wien, Geologische Specialkarte, Blatt 6557

Kloosterboer-van Hoeve ML, Steenbrink J, Visscher H, Brinkhuis H (2006) Millennial-scale climatic cycles in the Early Pliocene pollen record of Ptolemais, northern Greece. Palaeogeogr Palaeoclimatol Palaeoecol 229: 321–334

Kochansky-Devidé V, Slišković T (1978) Miocenske kongerije Hrvatske, Bosne i Hercegovine. Palaeontol Jugosl 19: 1–98

Krstić N, Savić Lj, Jovanović G, Bodor E (2003) Lower Miocene lakes of the Balkan Land. Acta Geol Hung 46:291–299

Mandic O, Harzhauser M, Pavelic D (2006) Cyclostratigraphy as a powerful evolutionist tool: case study from the Miocene of the Dinaride Ancient Lake System. Innsbruck University Press, Innsbruck, Pangeo, Austria 2006, Conference Series, pp 188–189

Mandic O, Harzhauser M, Pavelić D, de Leeuw A, Krijgsman W (2007) An integrative study of lacustrine successions of the Sinj Basin (Miocene Dinaride Lake System, SE Croatia)—paleontology, depositional history, cyclostratigraphy and paleomagnetics. Geophys Res Abstr 9:10331

Marinčić S, Korolija B, Majcen Ž., Borović I, Brkić M., Hrelić D, Magaš N, Benček Đ, Grimani I (1969) Omiš. Savezni geološki zavod, Beograd, Osnovna geološka karta Jugoslavije 1:100000

Meller B, Bergen PFv (2003) The problematic systematic position of Ceratostriatus Gregor (Hydracharitaceae ?)—morphological, anatomical and biochemical comparison with Stratiotes L. Plant Syst Evol 236:125–150

Monty CLV (1976) The origin and development of crypalgal fabrics. In: Walter MR (ed) Stromatolites, development in sedimentology, vol 20. Elsevier, Amsterdam, pp 447–477

Monty CLV, Hardie LA (1976) Geological significance of the freshwater blue-green algal calcareous marsh. In: Walter MR (ed) Stromatolites, development in sedimentology, vol 20. Elsevier, Amsterdam, pp 447–477

Monty CLV, Mass JR (1979) Lower Cretaceous (Wealden) blue green algal deposits of the province of Valencia (Spain). In: Monty CLV (ed) Phanerozoic stromatolites. Springer-Verlag, Berlin, pp 85–120

Neumayr M (1869) Beiträge zur Kenntniss fossiler Binnenfaunen. Jahrb Geol RA 19:355–382

Olujić J (1936) Ueber die geschlossenen, progressiven Entwicklungsreihen der Schalen der pontischen Prososthenien (Vorläufige Mitteilung). Arch Molluskenkd 68:118–120

Olujić J (1999) O razvojnim nizovima nekoliko melanopsida i prozostenida iz sarmatskih naslaga okolice Sinja (Dalmacija, Hrvatska). In: Jurišić-Polšak Z (ed) Josip Olujić. O razvojnim nizovima nekoliko melanopsida i prozostenida iz sarmatskih naslaga okolice Sinja (Dalmacija, Hrvatska). Hrvatski prirodoslovni muzej, Zagreb and Provincijalat Franjevačke provincije presvetog Otkupitelja, Sinj, pp 7–32, 33–60

Pamić J, McKee EH, Bullen T, Lanphere MA (1995) Tertiary volcanic rocks from Southern Pannonian basin, Croatia. Int Geol Rev 37:259–283

Papeš J, Marinković R, Raić V, Magaš N, Sikirica V (1984) Sinj. Savezni geološki zavod, Beograd Osnovna geološka karta Jugoslavije 1:100000

Pavelić D (2001) Tectonostratigraphic model for the North Croatian and North Bosnian sector of the Miocene Pannonian Basin System. Basin Res 13:359–376

Petrascheck W (1952) Der Einfluß der Fazies der Flözablagerung auf die Eigenschaften der Kohle. Z Dtsch Geol Ges 104:1–9

Pfleger V (1984) Schnecken und Muscheln Europas. Land und Süßwasserarten. Kosmos, Stuttgart

Platt NH, Wright VP (1991) Lacustrine carbonates: facies models, facies distributions and hydrocarbon aspects. In: Anadon P, Cabrera LI, Kelts K (eds) Lacustrine facies analysis. IAS, vol 13. Blackwell Scientific Publications, Oxford Special Publication, pp 57–74

Quedens G (1993) Strand und Wattenmeer. Tiere und Pflanzen an Nord- und Ostsee - ein Biotopführer. BLV, Münchenm Wien, Zürich

Raić V, Papeš J, Sikirica V, Magaš N (1984) Tumač za list Sinj K 33-10. Savezni geološki zavod, Beograd, Osnovna geološka karta Jugoslavije 1:100000

Rainer TM (2003) Thermal history and hydrocarbon potential of Carboniferous to Eocene sediments of the Alpine-Dinaric transition zone (Austria, Slovenia). Unpublished PhD thesis, University of Leoben

Rögl F, Coric S, Daxner-Höck H, Harzhauser M, Mandic O, Svábenická L, Zorn I (2004) Correlation of the Karpatian Stage. In: Brzobohatý R, Cicha I, Kovác M, Rögl F (eds) The Karpatian—a lower Miocene stage of the Central Paratethys. Masaryk University, Brno, pp 27–34

Rust J (1997) Evolution, Systematik, Paläoökologie und stratigraphischer Nutzen neogener Süß- und Brackwasser-Gastropoden im Nord-Ägäis-Raum. Palaeontogr Abt A 243:37–180

Schieber J (2002) Sedimentary pyrite: a window into the microbial past. Geology 30:531–534

Srdoč D, Horvatinčić N, Obelić B, Krajcar-Bronić I, Sliepčević A (1985) Procesi taloženja kalcita u krškim vodama s posebnim osvrtom na Plitvička jezera. Cars Iugosl 11(4–6):101–204

Stace C (1997) New Flora of the British Isles, 2nd edn. Cambridge University Press, Cambridge

Stoffers P (1975) Recent carbonate sedimentation in the lake of Plitvice (Yug.). Neues Jahrb Mineral Monatsh 1975(9): 412–418

Šušnjara A, Sakač K (1988) Miocene freshwater sediments of the Sinj area—Middle Dalmatia. Geol Vjesn 41:51–74

Šušnjara A, Šćavničar B (1974) Tuffs in Neogene deposits of Central Dalmatia (Southern Croatia). Geol Vjesn 27: 239–253

Sýkorová I, Pickel W, Christanis K, Wolf M, Taylor GH, Flores D (2005) Classification of huminite—ICCP Sytem 1994. Int J Coal Geo 62:85–106

Takšić A (1968) Die Vertebratenfaune aus dem Goručicatal bei Sinj. Bull sci Cons Acad Yougosl A 13:74–75

Talbot MR, Allen PA (1996) Lakes. In: Reading HG (ed) Sedimentary environments: processes, facies and stratigraphy, 3rd edn. Blackwell Science, Oxford, pp 83–124

Tari V (2002) Evolution of the northern and western Dinarides: a tectonostratigraphic approach. European Geosciences Union Stephan Mueller Special Publication Series 1: 223–236

Taylor H, Teichmüller M, Davis A, Diessel CFK, Littke R, Robert P (1998) Organic petrology. Borntraeger, Berlin-Stuttgart

Tucker EM, Wright VP (1990) Carbonate sedimentology. Blackwell, Oxford

Wheeler BR (2007) *Damasonium alisma* Miller. Plantlife International Species Dossier, Plantlife, Salisbury, UK

Wright VP (1985) Algal marsh deposits from the Upper Jurassic of Portugal. In: Toomey DF, Nitecki MH (eds) Paleoalgology: contemporary research and applications. Springer-Verlag, Berlin, pp 330–341

Žagar-Sakač A, Sakač K (1987) Novi nalazi fosilnih lopoča (Nymphaeaceae) u tercijarnim naslagama Dalmacije. Rad Jugosl Akad Znan Umjetn 431 Razr Prir Znan 22:207–218